# Strong Supernova 1987A Constraints on Bosons Decaying to Neutrinos

Damiano F. G. Fiorillo,[1] Georg G. Raffelt,[2] and Edoardo Vitagliano[3]
[1]*Niels Bohr International Academy, Niels Bohr Institute, University of Copenhagen, 2100 Copenhagen, Denmark*
[2]*Max-Planck-Institut für Physik (Werner-Heisenberg-Institut), Föhringer Ring 6, 80805 München, Germany*
[3]*Department of Physics and Astronomy, University of California, Los Angeles, California 90095-1547, USA*

(Received 28 September 2022; revised 17 January 2023; accepted 21 June 2023; published 13 July 2023)

Majoron-like bosons would emerge from a supernova (SN) core by neutrino coalescence of the form $\nu\nu \to \phi$ and $\bar{\nu}\bar{\nu} \to \phi$ with 100-MeV-range energies. Subsequent decays to (anti)neutrinos of all flavors provide a flux component with energies much larger than the usual flux from the "neutrino sphere." The absence of 100-MeV-range events in the Kamiokande-II and Irvine-Michigan-Brookhaven signal of SN 1987A implies that less than 1% of the total energy was thus emitted and provides the strongest constraint on the Majoron-neutrino coupling of $g \lesssim 10^{-9}$ MeV$/m_\phi$ for 100 eV $\lesssim m_\phi \lesssim$ 100 MeV. It is straightforward to extend our new argument to other hypothetical feebly interacting particles.

DOI: 10.1103/PhysRevLett.131.021001

*Introduction.*—The hot, dense cores of collapsing stars are powerful test beds for novel feebly interacting particles (FIPs), such as sterile neutrinos, dark photons, new scalars, axions, axionlike particles, and many others [1–3], notably including "secret" neutrino-neutrino interactions [4–8]. In standard supernova (SN) theory, the trapped electron-lepton number (some 0.30 per baryon) and the gravitational binding energy (some 10% of the formed neutron star's mass) are carried away by neutrinos on a timescale of a few seconds. The neutrino burst from the historical SN 1987A was observed in the Kamiokande-II [9–13] and Irvine-Michigan-Brookhaven (IMB) [14–16] water Cherenkov detectors and the Baksan underground scintillation telescope [17,18]. Despite sparse statistics and several anomalies, it has been taken to confirm the standard picture, leaving only limited room for energy loss in the form of FIPs.

If the FIPs interact so strongly that they are trapped themselves or decay before leaving the SN, they contribute to energy transfer [19] and may strongly affect overall SN physics and the explosion mechanism. A class of low-explosion-energy SNe provides particularly strong constraints on such scenarios [20]. FIPs on the trapping side of the SN-excluded regime are often constrained by other arguments, although allowed gaps may remain, such as the historical hadronic axion window or, more recently, the "cosmic triangle" for axionlike particles, both meanwhile closed.

Radiative decays en route to Earth and beyond provide strong limits using $\gamma$-ray observations from SN 1987A and the cosmic diffuse background [21–26]. Similar arguments pertain to kilonovae [27] and hypernovae [28].

In other cases, FIP decays include active neutrinos. In the free-streaming limit, FIPs escape from the inner SN core and so their decays provide 100-MeV-range events, much larger than the usual neutrino burst of few 10 MeV that emerges from the neutrino sphere at the edge of the SN core. The background of atmospheric muons has yet larger energies and so the new signal would stick out in a future SN neutrino observation. This argument was first advanced in Ref. [7] and offers an intriguing future detection opportunity.

Our main point is that, by the same token, SN 1987A already provides restrictive limits because the legacy data do not sport any events with such intermediate energies. This constraint, which is available today without the need to wait for the next galactic SN, is far more restrictive than the traditional energy-loss argument.

We illustrate our new argument with the simple case of nonstandard or secret neutrino-neutrino interactions [4–8], mediated by a (pseudo)scalar $\phi$ (mass $m_\phi$) that we call Majoron and take to interact with all flavors with the same strength $g$. We consider $m_\phi \gtrsim 100$ eV so that neutrino masses and refractive matter potentials can be ignored. The lepton-number violating production channels $\bar{\nu}\bar{\nu} \to \phi$ and $\nu\nu \to \phi$ and corresponding decays yield the constraints previewed in Fig. 1.

The older Majoron literature [31–39] instead took the low-mass limit where neutrino coalescence $\nu\bar{\nu} \to \phi$ and decay is enabled by the matter potential and, otherwise, second-order processes of the type $\nu\phi \to \nu\phi$ or $\nu\bar{\nu} \to \phi\phi$ dominate. One may consult Fig. 9 of Ref. [6] for the landscape of constraints, including previous SN 1987A energy-loss limits in our mass range [4,5].

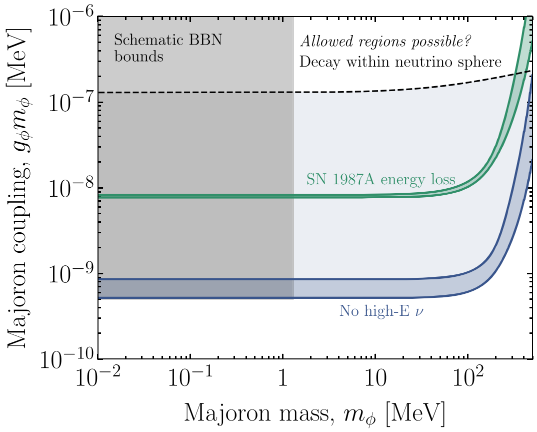


FIG. 1. Constraints on the Majoron coupling in the $m_\phi$–$g_\phi m_\phi$ plane from SN 1987A energy loss (green) and the absence of 100-MeV-range ("high-E") events (blue). The shaded range brackets the cold (upper curves) vs hot (lower curves) SN models, i.e., the Garching muonic models SFHo-18.8 and LS220-s20.0 [29]. Above the dashed line, Majorons with a reference kinetic energy of 110-MeV decay before leaving the SN core. The "ceiling" of the energy-loss bound is probably outside this figure, but we are not confident about its exact location. The schematic big bang nucleosynthesis (BBN) bounds are taken from Fig. 1 of Ref. [30], based on the cosmic radiation density. Somewhat more restrictive limits may follow from the cosmic microwave background (CMB) (see text).

*Majoron decay and production.*—A universal $\nu$–$\nu$ interaction by Majoron exchange is given by [39]

$$\mathcal{L}_{\rm int} = -\frac{g}{2}\psi_\nu^T\sigma_2\psi_\nu\phi + \text{H.c.}, \tag{1}$$

where $\psi_\nu$ is a two-component Majorana field and $g$ is a real number. In the relativistic limit, we refer to the Majorana helicity states as $\nu$ and $\bar\nu$ in the usual sense.

The decay into pairs of relativistic neutrinos requires equal helicities, implying the lepton-number violating channels $\phi \to \nu\nu$ or $\bar\nu\bar\nu$. Each individual rate is

$$\Gamma_{\phi\to\nu\nu} = \frac{g^2 m_\phi}{32\pi}, \tag{2}$$

which includes a symmetry factor 1/2 for identical final-state particles. (We always use natural units with $\hbar = c = k_B = 1$.) The total rate requires a factor of 6 for six species [40]. For a relativistic Majoron, this rate is slower by the Lorentz factor $m_\phi/E_\phi$, implying that the laboratory decay rate depends only on the combination $gm_\phi$.

The requirement that Majorons with $E_\phi = 100$ MeV decay beyond the neutrino-sphere radius of 20 km thus implies $gm_\phi \lesssim 10^{-7}$ MeV, shown as a dashed line in Fig. 1. On the other hand, the decay neutrinos should not be delayed by more than a few seconds. The requirement $\Gamma^{-1} \lesssim 1$ s implies $gm_\phi \gtrsim 1\times 10^{-9}$ MeV for $E_\phi = 100$ MeV. The time-of-flight difference is much smaller for relativistic Majorons, so for the constraints shown in Fig. 1 the signals are indeed contemporaneous, although somewhat marginally for $m_\phi$ around 100 MeV.

The neutrino decay spectrum is flat between $E_\pm = \frac{1}{2}(E_\phi \pm p_\phi)$ with $p_\phi = (E_\phi^2 - m_\phi^2)^{1/2}$. In a neutrino gas of one species $\alpha$, occupation number $f_\alpha(E_\nu)$, the spectral Majoron emission rate from $\nu_\alpha\nu_\alpha$ coalescence then is

$$\left.\frac{d\dot N_\phi^{(\alpha)}}{dE_\phi}\right|_{E_\phi} = \frac{g^2 m_\phi^2}{64\pi^3}\int_{E_-}^{E_+} dE_\nu f_\alpha(E_\nu) f_\alpha(E_\phi - E_\nu). \tag{3}$$

For local thermal equilibrium with temperature $T$ and neutrino chemical potential $\mu_\alpha$, the corresponding Fermi-Dirac distribution is $f_\alpha(E_\nu) = [e^{(E_\nu-\mu_\alpha)/T}+1]^{-1}$. The chemical potential for a flavor $\nu_\ell$ enters with opposite sign, depending on $\alpha$ denoting a $\nu$ or $\bar\nu$. Notice that the lepton-number violation caused by the $\phi$ interaction implies $\mu_\nu = 0$ in true equilibrium.

All Majorons decay close to the SN equally into all six neutrino species with a flat spectrum. Therefore, the effective single-species spectral neutrino emission rate is

$$\left.\frac{d\dot N_\alpha}{dE_\nu}\right|_{E_\nu} = \frac{2}{6}\int_{E_{\rm min}}^{\infty}\frac{dE_\phi}{p_\phi}\sum_{\beta=1}^{6}\left.\frac{d\dot N_\phi^{(\beta)}}{dE_\phi}\right|_{E_\phi}. \tag{4}$$

The minimal $E_\phi$ to produce a neutrino of energy $E_\nu$ is $E_{\rm min} = E_\nu + m_\phi^2/4E_\nu$. The first factor of 2 is for two neutrinos per decay, whereas 1/6 appears because this is the rate into one of six species.

*One-zone SN model.*—For a first estimate, we use a one-zone model of the collapsed SN core with a chemical potential $\mu_\nu = 100$ MeV for $\nu_e$ and vanishing for the other flavors, volume $(4\pi/3)R^3$ with $R = 10$ km for the emitting region, and duration for substantial deleptonization of $\tau = 1$ s [41]. After collapse, the SN core is cold ($T \simeq 10$ MeV) and heats up from outside in as the material deleptonizes. Majoron emission is thus from the coalescence of $\nu_e\nu_e$ alone, which we take as perfectly degenerate. (In contrast, novel particle emission usually becomes large only after the SN core has heated up at around 1 s after collapse [24].)

For $m_\phi = 0$, the integral in Eq. (3) is a "triangle function" that rises linearly to the value $\mu_\nu$ at $E_\phi = \mu_\nu$ and then decreases linearly to zero at $E_\phi = 2\mu_\nu$. The energy-loss rate per unit volume is $Q_\phi = (gm_\phi)^2\mu_\nu^3/64\pi^3$. Comparing $L_\phi = Q_\phi(4\pi/3)R^3$ with $L_\nu \simeq 2\times 10^{52}$ erg/s as recommended by a simple recipe [2] implies $gm_\phi \lesssim 4\pi\sqrt{3L_\nu/R^3\mu_\nu^3} = 5.5\times 10^{-9}$ MeV.

Likewise, the effective $\nu_\alpha$ production rate per unit volume is $\dot N_\alpha = (g^2 m_\phi^2/64\pi^3)\mu_\nu^2/3$ and therefore the total emitted number is $N_\alpha = \dot N_\alpha(4\pi/3)R^3\tau$. The fluence at Earth is $N_\alpha/(4\pi d_{\rm SN}^2)$ where $d_{\rm SN} = 49.6$ kpc is the distance to SN 1987A [66]. The largest detector was IMB with a fiducial mass of 6.8 kton [15] and thus $N_p = 4.5 \times 10^{32}$ fiducial protons. The detection cross section is very roughly $\sigma \simeq \bar{\sigma} E_\nu^2$ with $\bar{\sigma} \simeq 10^{-43}\ \mathrm{cm^2/MeV^2}$ and $\langle E_\nu^2 \rangle = 7\mu_\nu^2/18$. The total number of 100-MeV-range events therefore is $N_{e^+} = \sigma N_p N_\alpha / 4\pi d_{\rm SN}^2$ and the requirement $N_{e^+} \lesssim 1$ implies $g m_\phi \lesssim 72 (2 d_{\rm SN}^2 \pi^3 / 7 N_p R^3 \mu_\nu^4 \bar{\sigma} \tau)^{1/2} = 1 \times 10^{-9}$ MeV.

*Numerical SN models.*—This constraint is much more restrictive than from energy loss, motivating a detailed study. To this end, we use the Garching 1D models SFHo-18.8 and LS220-s20.0 that were evolved with the PROMETHEUS VERTEX code with six-species neutrino transport [67]. These muonic models were recently also used for other particle constraints [24,29]. With different final neutron-star masses and different equations of state, these models were taken to span the extremes of a cold and a hot case, reaching internal $T$ of around 40 vs 60 MeV. On the other hand, the initial $\mu_{\nu_e}$ profiles are much more similar, in both cases around 150 MeV in the center and a "lepton core" reaching up to around 10 km. The lepton number of the outer core layers is released within a few milliseconds after core bounce in the form of the prompt $\nu_e$ burst. More details about these models are provided in the Supplemental Material [42].

SN neutrinos follow a quasithermal spectrum that can be represented by a Gamma distribution [68–70]. We thus write the time-integrated spectrum in the form

$$\frac{dN_{\bar{\nu}_e}}{dE_\nu} = \frac{E_{\rm tot}}{6E_0^2} \frac{(1+\alpha)^{1+\alpha}}{\Gamma(1+\alpha)} \left(\frac{E_\nu}{E_0}\right)^\alpha e^{-(1+\alpha)E_\nu/E_0}, \qquad (5)$$

where $E_{\rm tot}$ is the total SN energy release, $E_0$ is the average $\bar{\nu}_e$ energy, $\alpha$ is a parameter that would be 2 for a Maxwell-Boltzmann distribution, and $\Gamma$ is the Gamma function, not to be confused with a Gamma distribution. The factor $1/6$ represents assumed flavor equipartition. The parameters are chosen such that $E_{\rm tot}$, $E_0 = \langle E_\nu \rangle$, and $\langle E_\nu^2 \rangle$ agree with the numerical spectrum.

The cold model releases $E_{\rm tot} = 1.98 \times 10^{53}$ erg. The exact impact of flavor oscillations on SN neutrinos is not yet fully understood. Averaging over all three $\bar{\nu}$ flavors, we find $E_0 = 12.7$ MeV and $\alpha = 2.39$. For the hot model, these parameters are $E_{\rm tot} = 3.93 \times 10^{53}$ erg, $E_0 = 14.3$ MeV, and $\alpha = 2.07$.

*SN 1987A cooling limit.*—The local Majoron energy loss follows from Eq. (3), which we correct for gravitational redshift through the tabulated lapse factors as described in Ref. [24]. In the cold model, we find a Majoron luminosity at 1 s postbounce of $L_\phi(1\ \mathrm{s}) = (g m_{\rm MeV})^2 6.46 \times 10^{68}$ erg/s, where $m_{\rm MeV} = m_\phi/\mathrm{MeV}$. According to the traditional SN 1987A cooling argument [2,24,71], we compare it with $L_\nu(1\ \mathrm{s}) = 4.40 \times 10^{52}$ erg/s, leading to $g m_\phi < 0.83 \times 10^{-8}$ MeV shown in Fig. 1. For larger masses, we include a cutoff for those Majorons that are produced with insufficient energy to escape the gravitational potential as explained in the Supplemental Material of Ref. [20]. The total emission is $E_\phi^{\rm tot} = (g m_{\rm MeV})^2 1.94 \times 10^{69}$ erg and nominally $E_\nu^{\rm tot} = E_\phi^{\rm tot}$ for $g m_\phi = 0.99 \times 10^{-8}$ MeV, practically identical to the luminosity comparison at 1 s.

For the hot model, we find $L_\phi(1\ \mathrm{s}) = (g m_{\rm MeV})^2 1.39 \times 10^{69}$ erg/s, to be compared with $L_\nu(1\ \mathrm{s}) = 8.29 \times 10^{52}$ erg/s, leading to $g m_\phi < 0.77 \times 10^{-8}$ MeV. Moreover, $E_\phi^{\rm tot} = (g m_{\rm MeV})^2 4.39 \times 10^{69}$ erg and $E_\nu^{\rm tot} = E_\phi^{\rm tot}$ for $g m_\phi = 0.93 \times 10^{-8}$ MeV. As seen from these numbers and Fig. 1, the constraints are very insensitive to the specific SN model and similar to the one-zone estimate.

*Neutrino detection.*—The main SN 1987A neutrino observations came from the water Cherenkov detectors Kamiokande-II (2.14 kton) [9–11] and IMB (6.8 kton) [14–16]. They observed events with energies up to 40 MeV via inverse beta decay $\bar{\nu}_e + p \to e^+ + n$, whereas elastic scattering on electrons is small (but dominates for solar $\nu_e$ detection). For our 100-MeV-range energies, charged current (CC) reactions on oxygen of the form $\bar{\nu}_e + \mathrm{O} \to e^+ + X$ and $\nu_e + \mathrm{O} \to e^- + Y$, with $X$ and $Y$ excited final-state nuclei, dominate for $E_\nu \gtrsim 70$ MeV. For energies above the muon production threshold ($m_\mu = 105.7$ MeV), the corresponding muonic CC processes also happen, especially of course for atmospheric neutrinos at yet larger energies. Muons quickly come to rest by ionization and produce "Michel $e^\pm$" with a characteristic spectrum ending at 53 MeV, half the muon mass. Below the muon Cherenkov threshold of about 160 MeV, they are termed "invisible muons." (For more details about these processes, see the Supplemental Material [42].)

Figure 2 shows the spectral fluence (time-integrated flux) for the standard SN neutrinos from the cold model, averaged

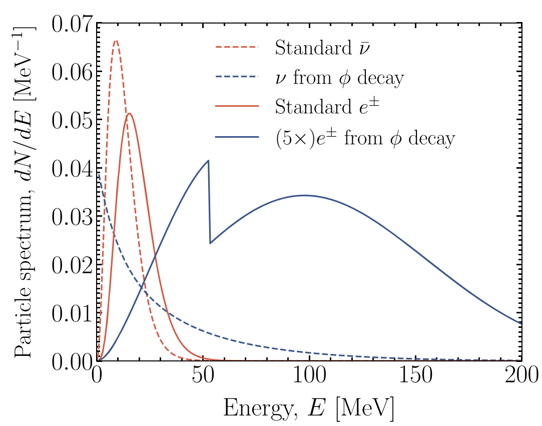


FIG. 2. Normalized particle spectra from the time-integrated emission of the cold model SFHo-18.8. "Standard $\bar{\nu}$" is the flavor average of the usual SN $\bar{\nu}$ and "Standard $e^\pm$" is the corresponding $e^\pm$ spectrum in the detector (ignoring detection efficiencies), whereas the new contributions are marked "from $\phi$ decay." They include Michel $e^\pm$ (end point 53 MeV) from $\mu^\pm$ decays at rest, which themselves emerge from CC interactions of $\nu_\mu$ and $\bar{\nu}_\mu$ that come from $\phi$ decay.

over $\bar{\nu}_e$, $\bar{\nu}_\mu$, and $\bar{\nu}_\tau$. The energy-integrated fluence is $5.10 \times 10^9\ \mathrm{cm}^{-2}$ for one species. We also show the corresponding $e^\pm$ spectrum in the detector; the total event number is 5.07 per kton (for 100% detection efficiency). Next we show the $\nu$ spectrum from $\phi$ decay, which is the same in every species; the total fluence in one species is $(gm_{\mathrm{MeV}})^2 1.90 \times 10^{25}\ \mathrm{cm}^{-2}$. The $e^\pm$ event number times $(gm_{\mathrm{MeV}})^2/\mathrm{kton}$ is $3.62 \times 10^{17}$, produced by $\bar{\nu}_e$ and $\nu_e$ in CC reactions and $0.37 \times 10^{17}$ from Michel $e^\pm$ ($E \lesssim 53$ MeV) caused by invisible muons, and a total of $3.99 \times 10^{17}$.

Above the muon Cherenkov threshold of 160 MeV, and assuming the same detection efficiency as for $e^\pm$, visible $\mu^\pm$ contribute another 11% to the total events. After each such event, the IMB detector would be blind by trigger dead time, so we should not include the subsequent Michel events. However, even for $\mu^\pm$ themselves, the Cherenkov threshold behavior and the detection efficiency are not available. Therefore, we do not include visible muons, making our Majoron bounds more conservative by some 5%.

A single event with 100% detection efficiency in IMB thus requires $gm_\phi = 6.06 \times 10^{-10}$ MeV. For the hot model, the corresponding result is $gm_\phi = 3.71 \times 10^{-10}$ MeV, both smaller than the estimate from the one-zone model, where we underestimated the cross section. Once more, the exact SN model is not crucial and we essentially find the limits shown in Fig. 1.

*Analysis of SN 1987A data.*—We now turn to a detailed analysis of the Kamiokande-II and IMB data. We summarize several details in the Supplemental Material [42] and here only remark that event information was recorded depending on a hardware trigger. In an off-line analysis, one searched for low-energy few-second event clusters. “Low energy” was defined in Kamiokande-II as less than 170 photoelectrons in the inner detector or $E_e \lesssim 50$ MeV [9–11], whereas IMB used maximally 100 photomultiplier tubes firing or $E_e \lesssim 75$ MeV [14–16]. However, as discussed in the Supplemental Material [42], we can conclude that no high-energy events were actually observed even above these thresholds during the SN 1987A burst.

The events from $\phi$ decay overlap with the standard SN signal, so one should perform a maximum likelihood analysis with $g$ and $m_\phi$ as fit parameters. However, the standard SN signal depends on the chosen SN model. For example, our cold (hot) model (using the average $\bar{\nu}_e - \bar{\nu}_\mu - \bar{\nu}_\tau$ spectrum) would have produced 9.12 (21.3) events in Kamiokande-II with average detected electron energy of 20.1 (22.6) MeV, to be compared with the actually observed 12 events with 14.7 MeV average energy. In IMB, they would have produced 3.49 (12.5) events on average with 31.3 (34.4) MeV, to be compared with 8 events with 31.9 MeV average. Neither of these models fits the data well and the Kamiokande-II and IMB data are themselves in tension with each other, although in terms of the $E_{\mathrm{tot}}$–$E_0$–$\alpha$ parameters one finds credible overlapping values [72,73].

We do not have a suite of SN models that would allow us to find the one that best fits the SN 1987A data. Instead we represent the signal in the form of Eq. (5) and use an unbinned likelihood for the energies of the events in each detector, as defined in the Supplemental Material [42]. First, we verify that the maximum of the likelihood for both experiments is at $g = 0$, i.e., neither of them prefers the new signal. Next, we marginalize the combined likelihood by maximizing it for each value of $g$ and $m_\phi$ over $E_0$ and $E_{\mathrm{tot}}$. This guarantees our constraints to be conservative, because for each choice of the Majoron parameters we choose the SN neutrino spectral shape as the one that maximizes the agreement with the data. We then follow the procedure outlined in Ref. [74] to set upper bounds on the Majoron coupling for each value of the Majoron mass; more details on our statistical procedure are given in the Supplemental Material [42]. We show the corresponding constraints, dominated by the IMB data, in Fig. 1.

*Discussion and outlook.*—We have considered FIPs that escape from the inner SN core and later decay into active neutrinos. Our main result is that the lack of 100-MeV-range events in the SN 1987A data provides surprisingly restrictive constraints. Specifically, the energy loss by $\nu\nu \to \phi$ Majoron emission must be less than 1% of the total binding energy, much more restrictive than the usual SN 1987A cooling limit.

Moreover, our new bound depends mainly on emission during the first second and not on the sparse late-time events or the predicted cooling speed that depends, e.g., on PNS convection. Our result is also insensitive to a concern that the SN 1987A neutron star has not yet been found (see, however, [75,76]) and that the late events could have been caused by black-hole accretion [77]. (See, however, [29] for a rebuttal of this scenario.)

Our limit implies that the impact on SN physics and the explosion mechanism is small. However, our discussion leaves open what happens for much stronger couplings when Majorons do not freely escape. The SN core could deleptonize already during infall, perhaps preventing a successful explosion. On the other hand, a thermal bounce may still occur [35,78]. If the interactions are yet stronger, neutrinos and Majorons form a viscous fluid that is more strongly coupled to itself than to the nuclear medium. This peculiar case was recently examined [8]; the SN 1987A signal may exclude a certain range of parameters beyond the upper edge of Fig. 1.

For $m_\phi \lesssim 1$ MeV, the cosmic radiation density measured by BBN provides comparable bounds (Fig. 1 of Ref. [30], see also Refs. [79–81]), and those from the CMB may be more restrictive, but the exact reach in mass and coupling strength was not directly provided. Having different systematic issues, the cosmological and SN 1987A arguments are nicely complementary for $m_\phi \lesssim 1$ MeV, whereas the SN 1987A sensitivity is unique for larger $m_\phi$.

Our method can be applied to any class of FIPs decaying to neutrinos. Examples include heavy neutral leptons [82,83] and gauge bosons arising from new symmetries like $U(1)_{L_\mu - L_\tau}$ [84,85], which can be further constrained relative to the existing bounds from energy loss [86,87]. Notice also that bosons coupling *exclusively* to neutrinos have different production rates if the coalescence process is lepton-number conserving ($\nu\bar{\nu} \to \phi$) or violating ($\nu\nu \to \phi$) because, in the PNS core, the neutrino and antineutrino distributions differ.

At present it remains open if there exist allowed Majoron parameters somewhere in the trapping regime, a question left for future study. Couplings below our limit leave open the exciting possibility of a detection in the neutrino signal of a future galactic SN [7] that would reveal FIP emission from the inner SN core.

We are indebted to M. Nakahata and T. Kajita for sharing unpublished information about the Kamiokande-II legacy data, and likewise J. Learned, J. LoSecco, and R. Svoboda for the analogous information about IMB. We thank H.-T. Janka and R. Bollig for providing the SN profiles used for our numerical estimates. G. R. acknowledges support by the German Research Foundation (DFG) through the Collaborative Research Centre "Neutrinos and Dark Matter in Astro and Particle Physics (NDM)," Grant No. SFB-1258, and under Germany's Excellence Strategy through the Cluster of Excellence ORIGINS EXC-2094-390783311. D. F. G. F. is supported by the Villum Fonden under Project No. 29388 and the European Union's Horizon 2020 Research and Innovation Program under the Marie Skłodowska-Curie Grant Agreement No. 847523 "INTERACTIONS." E. V. thanks the Niels Bohr Institute for hospitality and acknowledges support by the U.S. Department of Energy (DOE) Award No. DE-SC0009937, the Rosenfeld Foundation, and the Carlsberg Foundation (CF18-0183).

*Note added.*—Recently, our new argument was used to constrain the heavy-lepton model of Ref. [88].

[1] G. G. Raffelt, *Stars as Laboratories for Fundamental Physics* (University of Chicago Press, Chicago, 1996).
[2] G. G. Raffelt, Astrophysical axion bounds, Lect. Notes Phys. **741**, 51 (2008).
[3] L. Di Luzio, M. Fedele, M. Giannotti, F. Mescia, and E. Nardi, Stellar evolution confronts axion models, J. Cosmol. Astropart. Phys. 02 (2022) 035.
[4] L. Heurtier and Y. Zhang, Supernova constraints on massive (pseudo)scalar coupling to neutrinos, J. Cosmol. Astropart. Phys. 02 (2017) 042.
[5] T. Brune and H. Päs, Massive Majorons and constraints on the Majoron-neutrino coupling, Phys. Rev. D **99**, 096005 (2019).
[6] J. M. Berryman *et al.*, Neutrino self-interactions: A white paper, Phys. Dark Universe **42**, 101267 (2023).
[7] K. Akita, S. H. Im, and M. Masud, Probing non-standard neutrino interactions with a light boson from next Galactic and diffuse supernova neutrinos, J. High Energy Phys. 12 (2022) 050.
[8] P.-W. Chang, I. Esteban, J. F. Beacom, T. A. Thompson, and C. M. Hirata, Towards powerful probes of neutrino self-interactions in supernovae, arXiv:2206.12426.
[9] K. Hirata *et al.* (Kamiokande-II Collaboration), Observation of a Neutrino Burst from the Supernova SN1987A, Phys. Rev. Lett. **58**, 1490 (1987).
[10] K. S. Hirata *et al.*, Observation in the Kamiokande-II detector of the neutrino burst from supernova SN1987A, Phys. Rev. D **38**, 448 (1988).
[11] K. S. Hirata, Search for supernova neutrinos at Kamiokande-II, Ph.D. thesis, Tokyo University, 1991, https://lib-extopc.kek.jp/preprints/PDF/1991/9105/9105084.pdf, link to KEK repository.
[12] M. Koshiba, Observational neutrino astrophysics, Phys. Rep. **220**, 229 (1992).
[13] Y. Oyama, Re-examination of the time structure of the SN1987A neutrino burst data in Kamiokande-II, Astrophys. J. **922**, 223 (2021).
[14] R. M. Bionta *et al.*, Observation of a Neutrino Burst in Coincidence with Supernova SN 1987A in the Large Magellanic Cloud, Phys. Rev. Lett. **58**, 1494 (1987).
[15] C. B. Bratton *et al.* (IMB Collaboration), Angular distribution of events from SN1987A, Phys. Rev. D **37**, 3361 (1988).
[16] R. Svoboda *et al.* (IMB Collaboration), Neutrinos from Supernova 1987A in the IMB Detector, in: ESO Workshop on the SN 1987A, Garching, 1987, https://ui.adsabs.harvard.edu/abs/1987ESOC...26..229S.
[17] E. N. Alekseev, L. N. Alekseeva, V. I. Volchenko, and I. V. Krivosheina, Possible detection of a neutrino signal on 23 February 1987 at the Baksan underground scintillation telescope of the Institute of Nuclear Research, JETP Lett. **45**, 589 (1987).
[18] E. N. Alekseev, L. N. Alekseeva, I. V. Krivosheina, and V. I. Volchenko, Detection of the neutrino signal from SN 1987A in the LMC using the INR Baksan Underground Scintillation Telescope, Phys. Lett. B **205**, 209 (1988).
[19] A. Caputo, G. Raffelt, and E. Vitagliano, Radiative transfer in stars by feebly interacting bosons, J. Cosmol. Astropart. Phys. 08 (2022) 045.
[20] A. Caputo, H.-T. Janka, G. Raffelt, and E. Vitagliano, Low-Energy Supernovae Severely Constrain Radiative Particle Decays, Phys. Rev. Lett. **128**, 221103 (2022).
[21] M. Giannotti, L. D. Duffy, and R. Nita, New constraints for heavy axion-like particles from supernovae, J. Cosmol. Astropart. Phys. 01 (2011) 015.
[22] L. Oberauer, C. Hagner, G. Raffelt, and E. Rieger, Supernova bounds on neutrino radiative decays, Astropart. Phys. **1**, 377 (1993).
[23] J. Jaeckel, P. C. Malta, and J. Redondo, Decay photons from the axionlike particles burst of type II supernovae, Phys. Rev. D **98**, 055032 (2018).
[24] A. Caputo, G. Raffelt, and E. Vitagliano, Muonic boson limits: Supernova redux, Phys. Rev. D **105**, 035022 (2022).

[25] F. Calore, P. Carenza, M. Giannotti, J. Jaeckel, and A. Mirizzi, Bounds on axionlike particles from the diffuse supernova flux, Phys. Rev. D **102**, 123005 (2020).

[26] R. Z. Ferreira, M. C. D. Marsh, and E. Müller, Strong supernovae bounds on ALPs from quantum loops, J. Cosmol. Astropart. Phys. 11 (2022) 057.

[27] M. D. Diamond and G. Marques-Tavares, $\gamma$-Ray Flashes from Dark Photons in Neutron Star Mergers, Phys. Rev. Lett. **128**, 211101 (2022).

[28] A. Caputo, P. Carenza, G. Lucente, E. Vitagliano, M. Giannotti, K. Kotake, T. Kuroda, and A. Mirizzi, Axionlike Particles from Hypernovae, Phys. Rev. Lett. **127**, 181102 (2021).

[29] R. Bollig, W. DeRocco, P. W. Graham, and H.-T. Janka, Muons in Supernovae: Implications for the Axion-Muon Coupling, Phys. Rev. Lett. **125**, 051104 (2020); **126**, 189901(E) (2021).

[30] K. J. Kelly, M. Sen, and Y. Zhang, Intimate Relationship between Sterile Neutrino Dark Matter and ΔNeff, Phys. Rev. Lett. **127**, 041101 (2021).

[31] E. W. Kolb and M. S. Turner, Supernova 1987A and the secret interactions of neutrinos, Phys. Rev. D **36**, 2895 (1987).

[32] Y. Aharonov, F. T. Avignone, and S. Nussinov, Neutronization neutrino pulses from supernovae and the triplet Majoron model, Phys. Lett. B **200**, 122 (1988).

[33] Y. Aharonov, F. T. Avignone, and S. Nussinov, Implications of the triplet-Majoron model for the supernova SN1987A, Phys. Rev. D **37**, 1360 (1988).

[34] Y. Aharonov, F. T. Avignone, and S. Nussinov, Comment on "Constraints on the Majoron interactions from the supernova SN1987A", Phys. Rev. D **39**, 985 (1989).

[35] G. M. Fuller, R. Mayle, and J. R. Wilson, The Majoron model and stellar collapse, Astrophys. J. **332**, 826 (1988).

[36] J. A. Grifols, E. Masso, and S. Peris, Majoron couplings to neutrinos and SN1987A, Phys. Lett. B **215**, 593 (1988).

[37] K. Choi, C. W. Kim, J. Kim, and W. P. Lam, Constraints on the Majoron interactions from the supernova SN1987A, Phys. Rev. D **37**, 3225 (1988).

[38] K. Choi and A. Santamaria, Majorons and supernova cooling, Phys. Rev. D **42**, 293 (1990).

[39] Y. Farzan, Bounds on the coupling of the Majoron to light neutrinos from supernova cooling, Phys. Rev. D **67**, 073015 (2003).

[40] As in standard SN theory, "species" $\alpha$ denotes a state that could be $\nu$ or $\bar{\nu}$, whereas "flavor" denotes any of $\ell = e$, $\mu$, or $\tau$.

[41] These parameters are roughly calibrated by our cold numerical model. For the SN 1987A energy-loss argument [4] or future signal predictions for 100-MeV-range events [7], instead the values $\mu_\nu = 200$ MeV, $R = 10$ km, and $\tau = 10$ s were used, leading to overly restrictive limits and overly ambitious signal predictions (see Sec. E of the Supplemental Material [42]).

[42] See Supplemental Material at http://link.aps.org/supplemental/10.1103/PhysRevLett.131.021001 for further details about the detection cross sections for SN neutrinos in a water Cherenkov detector used in our analysis, the historical SN 1987A observations, our statistical analysis, and the Garching SN models. It includes Refs. [43–65].

[43] W. C. Haxton, The nuclear response of water Cherenkov detectors to supernova and solar neutrinos, Phys. Rev. D **36**, 2283 (1987).

[44] E. Kolbe, K. Langanke, and P. Vogel, Estimates of weak and electromagnetic nuclear decay signatures for neutrino reactions in Super-Kamiokande, Phys. Rev. D **66**, 013007 (2002).

[45] K. Scholberg, Supernova neutrino detection, Annu. Rev. Nucl. Part. Sci. **62**, 81 (2012).

[46] A. Strumia and F. Vissani, Precise quasielastic neutrino/nucleon cross-section, Phys. Lett. B **564**, 42 (2003).

[47] J. A. Formaggio and G. P. Zeller, From eV to EeV: Neutrino cross sections across energy scales, Rev. Mod. Phys. **84**, 1307 (2012).

[48] J. Marteau, J. Delorme, and M. Ericson, Neutrino oxygen interactions: Role of nuclear physics in the atmospheric neutrino anomaly, in *Proceedings of the 34th Rencontres de Moriond: Electroweak Interactions and Unified Theories* (Thế Giới Publishers, Vietnam, 1999), pp. 121–126, arXiv:hep-ph/9906449.

[49] K. Langanke, P. Vogel, and E. Kolbe, Signal for Supernova Muon-Neutrino and Tau-Neutrino Neutrinos in Water Cherenkov Detectors, Phys. Rev. Lett. **76**, 2629 (1996).

[50] IAUC 4316, http://www.cbat.eps.harvard.edu/iauc/04300/04316.html.

[51] N. Sanduleak, A deep objective-prism survey for Large Magellanic Cloud members, Contributions from the Cerro Tololo Inter-American Observatory (1970), Vol. **89**.

[52] R. M. Bionta *et al.* (IMB Collaboration), A Search for Proton Decay Into $e^+\pi^0$, Phys. Rev. Lett. **51**, 27 (1983); **51**, 522(E) (1983).

[53] https://www.nist.gov/pml/time-and-frequency-division/time-distribution/radio-station-wwvb.

[54] J. C. van der Velde, Possible evidence for a new particle from SN 1987A, Phys. Rev. D **39**, 1492 (1989).

[55] G. Raffelt, Horizontal branch stars and the neutrino signal from SN 1987A, Phys. Rev. D **38**, 3811 (1988).

[56] K. Arisaka *et al.*, Search for nucleon decay into charged lepton + mesons, J. Phys. Soc. Jpn. **54**, 3213 (1985).

[57] T. Kajita, M. Koshiba, and A. Suzuki, On the origin of the Kamiokande experiment and neutrino astrophysics, Eur. Phys. J. H **37**, 33 (2012).

[58] G. Badino *et al.*, The 90 ton liquid scintillator detector in the Mont Blanc laboratory, Nuovo Cimento Soc. Ital. Fis. **7C**, 573 (1984).

[59] M. Aglietta *et al.*, On the event observed in the Mont Blanc Underground Neutrino observatory during the occurrence of Supernova 1987a, Europhys. Lett. **3**, 1315 (1987).

[60] R. Schaeffer, Y. Declais, and S. Jullian, The neutrino emission of SN1987A, Nature (London) **330**, 142 (1987).

[61] I. Tamborra, F. Hanke, H.-T. Janka, B. Müller, G. G. Raffelt, and A. Marek, Self-sustained asymmetry of lepton-number emission: A new phenomenon during the supernova shock-accretion phase in three dimensions, Astrophys. J. **792**, 96 (2014).

[62] A. Burrows and J. M. Lattimer, The birth of neutron stars, Astrophys. J. **307**, 178 (1986).

[63] J. A. Pons, S. Reddy, M. Prakash, J. M. Lattimer, and J. A. Miralles, Evolution of proto-neutron stars, Astrophys. J. **513**, 780 (1999).

[64] S. W. Li, L. F. Roberts, and J. F. Beacom, Exciting prospects for detecting late-time neutrinos from core-collapse supernovae, Phys. Rev. D **103**, 023016 (2021).

[65] A. Pascal, J. Novak, and M. Oertel, Proto-neutron star evolution with improved charged-current neutrino-nucleon interactions, Mon. Not. R. Astron. Soc. **511**, 356 (2022).

[66] G. Pietrzyński *et al.*, A distance to the Large Magellanic Cloud that is precise to one per cent, Nature (London) **567**, 200 (2019).

[67] Garching core-collapse supernova research archive, https://wwwmpa.mpa-garching.mpg.de/ccsnarchive/.

[68] M. T. Keil, G. G. Raffelt, and H.-T. Janka, Monte Carlo study of supernova neutrino spectra formation, Astrophys. J. **590**, 971 (2003).

[69] I. Tamborra, B. Müller, L. Hüdepohl, H.-T. Janka, and G. Raffelt, High-resolution supernova neutrino spectra represented by a simple fit, Phys. Rev. D **86**, 125031 (2012).

[70] E. Vitagliano, I. Tamborra, and G. Raffelt, Grand unified neutrino spectrum at earth: Sources and spectral components, Rev. Mod. Phys. **92**, 045006 (2020).

[71] Scaling the original axion bounds to the Majoron case with that simple recipe ignores that here the particle emission is largest directly after core bounce, whereas in the axion or similar cases, the core first has to heat up and the emission is largest perhaps around 1 s postbounce. Moreover, Majorons remove both energy and lepton number. We suspect that the impact on the SN 1987A neutrino signal would be larger than implied by scaling the axion case. A detailed analysis would require including Majoron losses in self-consistent SN models. In view of the much more restrictive counting-rate argument, this exercise is not needed and we can postprocess existing models.

[72] B. Jegerlehner, F. Neubig, and G. Raffelt, Neutrino oscillations and the supernova SN1987A signal, Phys. Rev. D **54**, 1194 (1996).

[73] A. Mirizzi and G. G. Raffelt, New analysis of the SN 1987A neutrinos with a flexible spectral shape, Phys. Rev. D **72**, 063001 (2005).

[74] G. Cowan, K. Cranmer, E. Gross, and O. Vitells, Asymptotic formulae for likelihood-based tests of new physics, Eur. Phys. J. C **71**, 1554 (2011); **73**, 2501(E) (2013).

[75] P. Cigan *et al.*, High angular resolution ALMA images of dust and molecules in the SN 1987A ejecta, Astrophys. J. **886**, 51 (2019).

[76] D. Page, M. V. Beznogov, I. Garibay, J. M. Lattimer, M. Prakash, and H.-T. Janka, NS 1987A in SN 1987A, Astrophys. J. **898**, 125 (2020).

[77] N. Bar, K. Blum, and G. D'Amico, Is there a supernova bound on axions?, Phys. Rev. D **101**, 123025 (2020).

[78] M. Rampp, R. Buras, H.-T. Janka, and G. Raffelt, Core-collapse supernova simulations: Variations of the input physics, arXiv:astro-ph/0203493.

[79] G.-Y. Huang, T. Ohlsson, and S. Zhou, Observational constraints on secret neutrino interactions from big bang nucleosynthesis, Phys. Rev. D **97**, 075009 (2018).

[80] N. Blinov, K. J. Kelly, G. Z. Krnjaic, and S. D. McDermott, Constraining the Self-Interacting Neutrino Interpretation of the Hubble Tension, Phys. Rev. Lett. **123**, 191102 (2019).

[81] M. Escudero and S. J. Witte, A CMB search for the neutrino mass mechanism and its relation to the Hubble tension, Eur. Phys. J. C **80**, 294 (2020).

[82] G. M. Fuller, A. Kusenko, and K. Petraki, Heavy sterile neutrinos and supernova explosions, Phys. Lett. B **670**, 281 (2009).

[83] G. Magill, R. Plestid, M. Pospelov, and Y.-D. Tsai, Dipole portal to heavy neutral leptons, Phys. Rev. D **98**, 115015 (2018).

[84] R. Foot, New physics from electric charge quantization?, Mod. Phys. Lett. A **06**, 527 (1991).

[85] X.-G. He, G. C. Joshi, H. Lew, and R. R. Volkas, Simplest $Z'$ model, Phys. Rev. D **44**, 2118 (1991).

[86] M. Escudero, D. Hooper, G. Krnjaic, and M. Pierre, Cosmology with a very light $L_\mu - L_\tau$ gauge boson, J. High Energy Phys. 03 (2019) 071.

[87] D. Croon, G. Elor, R. K. Leane, and S. D. McDermott, Supernova muons: New constraints on $Z$' bosons, axions and ALPs, J. High Energy Phys. 01 (2021) 107.

[88] V. Brdar, A. de Gouvêa, Y.-Y. Li, and P. A. N. Machado, Neutrino magnetic moment portal and supernovae: New constraints and multimessenger opportunities, Phys. Rev. D **107**, 073005 (2023).